Seminar on Spatial Information Retrieval, Analysis, Reasoning and Modelling
18ᵗʰ-20ᵗʰ March 2009. ISI-DRTC, Bangalore, India

98

AUTOMATIC PIXEL CLASSIFICATION IN REMOTE SENSING SATELLITE IMAGERY USING A NEW MULTIOBJECTIVE SIMULATED ANNEALING BASED CLUSTERING TECHNIQUE

Sriparna Saha and Sanghamitra Bandyopadhyay

Machine Intelligence Unit, Indian Statistical Institute, Kolkata-700108, India.
Corresponding Authors' E-mail: {sriparna r,sanghamig@isical.ac.in}

Abstract— An important approach for unsupervised landcover classification in remote sensing images is the clustering of pixels in the spectral domain into several partitions. In this paper, a multiobjective optimization algorithm is utilized to tackle the problem of partitioning where a number of different cluster validity indices are simultaneously optimized. New multiobjective clustering algorithm uses the newly developed simulated annealing based multiobjective optimization technique (AMOSA) as the underlying optimization criterion. Here, center based encoding is used. Each cluster is divided into several small hyperspherical subclusters and the centers of all these small sub-clusters are encoded in a string to represent the whole cluster. For assigning points to different clusters these sub-clusters are considered individually. But for the purpose of objective function evaluation, these sub-clusters are merged appropriately to form some variable number of whole clusters. Two objective functions, one reflecting the total compactness of the partitionings based on the Euclidean distance, and another reflecting the total symmetrical compactness of the obtained partitioning are considered here. These are optimized simultaneously using AMOSA to detect the appropriate number of clusters and the appropriate partitioning from remote sensing image data sets. A new method is also developed to determine a single solution from the final Pareto optimal front provided by the newly developed multiobjective clustering technique (multicenter-AMOSA). Different landcover regions in remote sensing imagery have also been classified using the proposed technique to establish its efficiency. Results are compared with those obtained by fuzzy C-means (FCM) clustering technique and a recently developed symmetry based automatic clustering technique, VGAPS, both qualitatively and quantitatively.

1 INTRODUCTION

Remote sensing satellite images have significant applications in different areas such as climate studies, assessment of forest resources, examining marine environments, etc. An important task in remote sensing applications is the classification of pixels in the images into homogeneous regions, each of which corresponds to some particular landcover type. This problem has often been modeled as a clustering problem Bensaid et al. (1996) Maulik and Bandyopadhyay (2003) Saha and Bandyopadhyay (2007). However since it is difficult to have *a priori* information about the number of clusters in satellite images, the clustering algorithms should be able to automatically determine this value. Moreover, in satellite images it is often the case that some regions occupy only a few pixels, while the neighboring regions are significantly large. Thus automatically detecting regions or clusters of such widely varying sizes presents a challenge in designing clustering algorithms and validity indices.

The aim of any clustering technique is to evolve a partition matrix $U(X)$ representing a possible grouping of the given data set $X = \{x_1, x_2, \cdots, x_n\}$, into a number, say *K*, of clusters such that patterns in the same group are similar in some sense and patterns in different groups are dissimilar in the same sense. The partition matrix $U(X)$ of size $K \times n$ may be represented as $U = [u_{ik}], 1 \le i \le K; 1 \le k \le n$, where u_{ik} can take either the value `0' or the value `1'. $u_{ik} = 1$ denotes that the pattern x_k belongs to cluster $C_i (i = 1, \cdots, K)$ otherwise $u_{ik} = 0$ denotes that the pattern x_k does not belong to cluster $C_i (i = 1, \cdots, K)$.

Recently, the application of genetic algorithms (GAs) Goldberg (1989) in the field of pixel classification has attracted the attention of researchers Maulik and Bandyopadhyay (2003) Saha and Bandyopadhyay (2007). These techniques use a single cluster validity measure as the fitness function to reflect the goodness of an encoded clustering. However, a single cluster validity measure is seldom equally applicable for different kinds of data sets with different characteristics. Hence, it is necessary to simultaneously optimize several validity measures that can capture the different data characteristics. In order to achieve this, in this paper, the problem of automatic partitioning is posed as one of the multiobjective optimizations (MOOs) Deb (2001), where a search is performed over a number of, often conflicting, objective functions. The final solution set contains a number of Pareto optimal solutions, none of which can be further improved on any one objective without degrading it in another.

In this paper thus we have developed a new multiobjective simulated annealing based clustering technique which can automatically detect the appropriate number of clusters and the appropriate partitioning from image data sets with any type of clusters having

either symmetrical shape or well-separated structures. A newly developed simulated annealing based multiobjective optimization technique, AMOSA is used as the underlying optimization criterion. Here center based encoding as in Ref. Maulik and Bandyopadhyay (2000) is used. But as center based encoding prefers formation of hyperspherical shaped clusters, the concept of \multiple center" corresponding to each cluster is used in this article. Here each cluster is divided into several non-overlapping small hyperspherical sub-clusters and the centers of these sub-clusters are encoded in a string to represent a particular cluster. Two cluster validity indices are optimized simultaneously using the search capability of AMOSA. One of these cluster validity indices reects the total compactness of a particular partitioning and another one represents the total symmetry present in a particular partitioning. Any multiobjective optimization technique generates a large number of non-dominated solutions on its final Pareto optimal front. Each of these solutions provides a way of partitioning the particular data set. All these solutions are equally important from the algorithmic point of view, but sometimes user wants a single solution. Thus in this article we have also developed a new semi-supervised method to identify a single solution from the set of final Pareto optimal solutions. The superiority of the proposed multicenter-AMOSA to automatically segment different land cover types in comparison with point symmetry based automatic genetic clustering technique (VGAPS-clustering) and fuzzy C-means (FCM) clustering technique are shown for two remote sensing satellite images of the parts of the cities of Kolkata and Mumbai. Results are compared both quantitatively and qualitatively.

2. THE SA BASED MOO ALGORITHM: AMOSA

Archived multiobjective simulated annealing (AMOSA) Bandyopadhyay et al. (2008) is a generalized version of the simulated annealing (SA) algorithm based on multiobjective optimization (MOO). MOO is applied when dealing with the real-world problems where there are several objectives that should be optimized simultaneously. In general, a MOO algorithm usually admits a set of solutions that are not dominated by any solution it encountered, i.e., non-dominated solutions Deb (2001). During recent years, many multiobjective evolution algorithms, such as multiobjective EA (MOEA), have been suggested to solve the MOO problems Veldhuizen and Lamont (2000).

Simulated annealing (SA) is a search technique for solving difficult optimization problems, which is based on the principles of statistical mechanics Kirkpatrik *et al.* (1983). Recently, SA has become very popular because not only can SA replace the exhaustive search to save time and resource, but also converge to the global optimum if annealed sufficiently slowly Geman and Geman (1984).

Although the single objective version of SA is quite popular, its utility in the multiobjective case was limited because of its search-from-a-point nature. Recently Bandyopadhyay et al. developed an efficient multiobjective version of SA called AMOSA Bandyopadhyay *et al.* (2008) that overcomes this limitation. AMOSA is utilized in this

work for partitioning a data set.

    The AMOSA algorithm incorporates the concept of an archive where the non-dominated solutions seen so far are stored. Two limits are kept on the size of the archive: a hard or strict limit denoted by *HL*, and a soft limit denoted by *SL*. The algorithm begins with the initialization of a number $\left(\gamma \times SL, \gamma > 1\right)$ of solutions each of which represents a state in the search space. The multiple objective functions are computed. Each solution is refined by using simple hill-climbing and domination relation for a number of iterations. Thereafter the non-dominated solutions are stored in the archive until the size of the archive increases to *SL*. If the size of the archive exceeds *HL*, a single-linkage clustering scheme is used to reduce the size to *HL*. Then, one of the points is randomly selected from the archive. This is taken as the current-pt, or the initial solution, at temperature $T = T_{\max}$. The current-pt is perturbed to generate a new solution named new-pt, and its objective functions are computed. The domination status of the new-pt is checked with respect to the current-pt and the solutions in the archive. A new quantity called amount of domination, $\Delta dom\left(a,b\right)$ between two solutions a and b is defined as follows:

$$\Delta dom\left(a,b\right) = \prod_{i=1, f_i(a) \neq f_i(b)}^{M} \frac{f_i\left(a\right) - f_i\left(b\right)}{R_i},$$

where $f_i\left(a\right)$ and $f_i\left(b\right)$ are the *i*th objective values of the two solutions and R_i is the corresponding range of the objective function. Based on domination status different cases may arise viz., accept the (i) new-pt, (ii) current-pt, or, (iii) a solution from the archive. Again, in case of overflow of the archive, clustering is used to reduce its size to HL. The process is repeated *iter* times for each temperature that is annealed with a cooling rate of $\alpha\left(<1\right)$ till the minimum temperature $T_{\min}$ is attained. The process thereafter stops, and the archive contains the final non-dominated solutions.

    It has been demonstrated in Ref.Bandyopadhyay *et al*. (2008) that the performance of AMOSA is better than that of NSGA-II Deb *et al*. (2002) and some other well-known MOO algorithms.

3. PROPOSED METHOD OF MULTIOBJECTIVE CLUSTERING

In this paper a new multiobjective clustering technique, multicenter-AMOSA, is proposed which uses a newly developed multiobjective simulated annealing based method, AMOSA Bandyopadhyay *et al*. (2008) as the underlying optimization technique.

3.1 String Representation and Population Initialization
In AMOSA based clustering, the strings are made up of real numbers which represent the

coordinates of the centers of the partitions. AMOSA attempts to evolve an appropriate set of cluster centers that represent the associated partitioning of the data. Here for the purpose of encoding multi-center approach is used. Each cluster is divided into several small non-overlapping hyperspherical sub-clusters. Then each cluster is represented by the centers of these individual sub-clusters. Suppose a particular string encodes the centers of *K* number of clusters and each cluster is divided into *C* number of sub-clusters. If the data set is of dimension *d*, then the length of the string is $C \times K \times d$.

This concept of representing one cluster using multi-center is shown in Figure 1. Suppose a particular string contains $K = 2$ number of clusters. Each cluster is divided into 10 small sub-clusters, i.e., here $C = 10$. Let the dimension(*d*) of the data set be 2. Suppose the center of the *j*th sub-cluster is denoted by $\bar{c}_j = (cx_j, cy_j)$. Then this string will look like: $< cx_i, cy_i, cx_2, cy_2, \cdots, cx_{20}, cy_{20} >$. Each string *i* in the archive initially contains K_i number of clusters, such that $K_i = (rand() \bmod (K^{max} - 1)) + 2$.. Here, $rand()$ is a function returning an integer, and K^{max} is a soft estimate of the upper bound of the number of clusters. The number of clusters will therefore range from two to K^{max}. For a particular string in the archive, first the initial K_i number of cluster centers are selected. Using the *K*-means like cluster assignment, each cluster is formed. Then *C* number of distinct points are selected from each cluster randomly. These $C \times K_i$ number of points are encoded in that particular string. Corresponding to each string a partition matrix of size $(C \times K_i) \times n$ is kept.
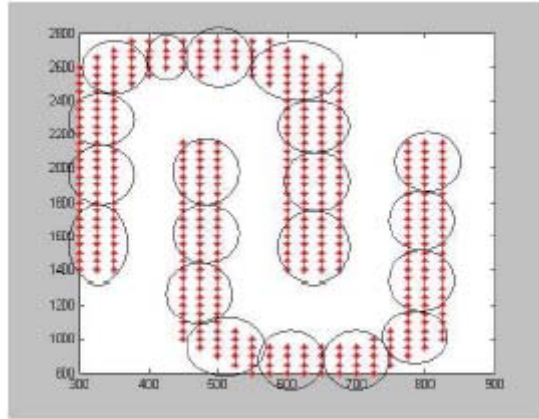
Figure 1. Example of representing a single cluster using multiple cluster centers.

3.2 Assignment of Points

For the purpose of assignment, each sub-cluster is considered as a separate cluster. Here assignment is done based on the minimum Euclidean distance criterion as done in normal

K-means clustering technique Everitt (1993). A particular data point $\bar{x}_j$ is assigned to the kth sub-cluster where

$$k = \arg\min_{i=1}^{K \times C} d_e\left(\bar{c}_i, \bar{x}_j\right).$$

Thereafter, the partition matrix is formed in the following way: $u(kj) = 1$ and $u(ij) = 0, \forall i = 1 \cdots K \times C, k \neq i.$

3.3 Objective Functions Used

For the optimization purpose, two different cluster validity indices are considered. These two objective functions reflect two different aspects of good clustering solutions. The first one quantifies the amount of symmetry present in a particular partitioning. And the second one measures the compactness of the partitionings in terms of the Euclidean distance. These indices are described below.

3.3.1 Cluster Validity Index Based on Symmetry:

Sym-index. This cluster validity index is based on a newly developed point symmetry (PS) based distance Bandyopadhyay and Saha (2007).

The PS distance Bandyopadhyay and Saha (2007), $d_{ps}\left(\bar{x}, \bar{c}\right)$, associated with point

$\bar{x}$ with respect to a center $\bar{c}$ is calculated as follows. Let a point be $\bar{x}$. The symmetrical

(reflected) point of $\bar{x}$ with respect to a particular center $\bar{c}$ is $2 \times \bar{c} - \bar{x}$. Let us denote

this by $\bar{x}^*$. Let *knear* unique nearest neighbors of $\bar{x}^*$ be at Euclidean distances of
$d_i s, i = 1, 2, \cdots knear$. Then

$$d_{ps}\left(\bar{x}, \bar{c}\right) = d_{sym}\left(\bar{x}, \bar{c}\right) \times d_e\left(\bar{x}, \bar{c}\right), \qquad (1)$$

$$= \frac{\sum_{i-1}^{knear} d_i}{knear} \times d_e\left(\bar{x}, \bar{c}\right), \qquad (2)$$

where $d_e\left(\bar{x}, \bar{c}\right)$ is the Euclidean distance between the point $\bar{x}$ and $\bar{c}$, and $d_{sym}\left(\bar{x}, \bar{c}\right)$

is a symmetry measure of $\bar{x}$ with respect to $\bar{c}$. It can be seen from Equation 2 that *knear*

cannot be chosen equal to 1, since if $\bar{x}^*$ exists in the data set then $d_{ps}\left(\bar{x}, \bar{c}\right) = 0$ and

hence there will be no impact of the Euclidean distance. On the contrary, large values of
knear may not be suitable because it may underestimate the amount of symmetry of a
point with respect to a particular cluster center. Here knear is chosen equal to 2. It may be
noted that the proper value of *knear* largely depends on the distribution of the data set. A
fixed value of *knear* may have many drawbacks. For instance, for very large clusters (with
too many points), 2 neighbors may not be enough as it is very likely that a few neighbors
would have a distance close to zero. On the other hand, clusters with too few points are
more likely to be scattered, and the distance of the two neighbors may be too large. Thus a
proper choice of *knear* is an important issue that needs to be addressed in the future.

Note that $d_{ps}\left(\bar{x}, \bar{c}\right)$, which is a non-metric, is a way of measuring the amount of

point symmetry between a point and a cluster center, rather than the distance like any
Minkowski distance.

Sym-index Bandyopadhyay and Saha (2008) is a cluster validity function which
measures the overall average symmetry with respect to the cluster centers. Consider a

partition of the image data set $X = \left\{ x_j : j = 1, 2, \cdots, n \right\}$ K clusters where the center of

cluster $\bar{c}$ is computed by using $\bar{c} = \dfrac{\sum_{j=1}^{n_i} \bar{x}_j^i}{n_i}$, where $n_i = (i = 1, 2, \cdots, K)$ is the

number of points in cluster i and $\bar{x}_j^i$ denotes the jth point of the ith cluster. The new cluster validity function *Sym* is defined as:

$$Sym(K) = \left(\frac{1}{K} \times \frac{1}{\varepsilon_K} \times D_K \right). \tag{3}$$

Here,

$$\varepsilon_K = \sum_{i=1}^{K} E_i, \tag{4}$$

such that

$$E_i = \sum_{i=1}^{K} d_{ps}^* \left(\bar{x}_j^i, \bar{c}_i \right) \tag{5}$$

and

$$D_K = \max_{i,j=1}^{K} \left\| \bar{c}_i - \bar{c}_j \right\| \tag{6}$$

D_K is the maximum Euclidean distance between two cluster centers among all pairs of

centers. $d_{ps}^* \left(\bar{x}_j^i, \bar{c}_i \right)$ is computed by Equation 2 with some constraint. Here, the first

knear nearest neighbors of $\bar{x}_j^* = 2 \times \bar{c}_i - \bar{x}_j^i$ will be searched among only those points

which are in cluster i, i.e., the *knear* nearest neighbors of $\bar{x}_j^*$, the reflected point of $\bar{x}_j^i$

with respect to $\bar{c}_i$, and $\bar{x}_j^i$ should belong to the ith cluster. The objective is to maximize this index in order to obtain the actual number of clusters.

    As formulated in Equation 3, *Sym*-index is a composition of three factors, $\dfrac{1}{k}, \dfrac{1}{\varepsilon_K}$

and D_K. The first factor increases as K decreases; as *Sym*-index needs to be maximized for optimal clustering, this factor prefers to decrease the value of K. The second factor is a measure of the total within cluster symmetry. For clusters which have good symmetrical structures, ε_K value is less. Note that as K increases, in general, the clusters tend to become more symmetric. Moreover, as $d_e\left(\overline{x},\overline{c}\right)$ in Equation 2 also decreases, ε_K decreases, resulting in an increase in the value of the *Sym*-index. Since *Sym*-index needs to be maximized, it will prefer to increase the value of K. Finally the third factor, D_K, measuring the maximum separation between a pair of clusters, increases with the value of K. Note that the value of D_K is bounded by the maximum separation between a pair of points in the data set. As these three factors are complementary in nature, so they are expected to compete and balance each other critically for determining the proper partitioning.

3.3.2 Euclidean Distance Based Cluster Validity Index: I-index.
The second objective function used here is a well-known Euclidean distance based cluster validity index, *I*-index Maulik and Bandyopadhyay (2002). It is defined as follows:

$$I(K) = \left(\frac{1}{K} \times \frac{E_1}{E_K} \times D_K \right)^p,$$

where K is the number of clusters. Here $E_K = \sum_{k=1}^{K} \sum_{j=1}^{n_k} d_e\left(\overline{c}_k, \overline{x}_j^k \right)$ and

$D_K = \max_{i,j=1}^{K} d_e\left(\overline{c}_i, \overline{c}_j \right)$ where $\overline{c}_j$ denotes the center of the *j*th cluster and $\overline{x}_j^k$

denotes the *j*th point of the *k*th cluster. n_k is the total number of points present in the *k*th cluster. The value of K for which *I*-index takes its maximum value is considered as the appropriate number of clusters. The index *I* is a composition of three factors, namely, $\frac{1}{K}, \frac{E_1}{E_K}$ and D_K. The first factor will try to reduce index *I* as K is increased. The second factor consists of the ratio of E_1, which is constant for a given data set, and E_K, which decreases with increase in K. Hence, because of this term, index *I* increases as E_K decreases. This, in turn, indicates that formation of more numbers of clusters, which are

compact in nature, would be encouraged. Finally, the third factor, D_K (which measures the maximum separation between two clusters over all possible pairs of clusters), will increase with the value of *K*. However, note that this value is upper bounded by the maximum separation between two points in the data set. Thus, the three factors are found to compete with and balance each other critically. The power *p* is used to control the contrast between the different cluster configurations. In this article, we have taken *p* = 2.

```
Begin
    1. for i=1:K,
        set_i = ∅
    end for
    2. for j = 1 : K × C,
        flag(i)=1
    end
    3. for i=1:K,
        {min_entry1, min_entry2}=argmin_{i,j=1,i≠j,flag(i)=1∧flag(j)==1}^{C×K} distance(i,j)
        set_i = set_i ⋃{min_entry1, min_entry2}
        flag(min_entry1)=0, flag(min_entry2)=0
        for j=1:C-2,
            min_entry3=argmin{min_{p∈set_i} min_{q=1∧flag(q)=1}^{C×K} distance(p,q)}
            set_i = set_i ⋃{min_entry3}
            flag(min_entry3)=0;
        end for
    end for
    Merge the points which are assigned to any of the cluster centers present in set_i
to form the ith cluster, i.e.,
    suppose C_i denotes the set of points of the ith cluster
    then, C_i = {x̄_j : 1 ≤ j ≤ n ∧ u_jm = 1 where m ∈ Set_i}.
End
```

Figure 2. Merging of Cluster Centers in *multicenter-AMOSA*.

3.3.3 Objective Function Calculation.

Before computing the above mentioned two objective functions for each string, at first total $C \times K$ number of sub-clusters encoded in a particular string are merged to form total *K* number of clusters. The merging operation is done in the following way. First, the distance between each pair of cluster centers is computed. Suppose this distance matrix is denoted as *distance*, i.e.,

$$dis\tan ce = \left[d\left(c_i, c_j\right) \right]_{i,j=1...C\times K}.$$

Here $d\left(c_i, c_j\right)$ denotes the Euclidean distance between two cluster centers c_i and c_j.
Then the merging operation is carried out following the procedure described in Figure 2.

After the merging operation is done, new cluster centers for these *K* clusters are formed as follows:

$$c_k = \frac{\sum_{\bar{x}\in C_K} \bar{x}}{n_k},$$

where n_k is the total number of points in the *k*th cluster. Two cluster validity indices are computed for each string. Then the objective functions for a particular string are:

$$obj = \left\{sym\left(K\right), I\left(K\right)\right\}$$

where *sym(K)* and *I(K)* are, respectively, the calculated *Sym*-index value, and *I*-index value for that particular string. Here *K* denotes the number of clusters present in that particular string. These two objective functions are simultaneously maximized by using the simulated annealing based MOO algorithm, AMOSA.

3.4 Mutation Operation
A new string is generated from the current one by adopting one of the following three types of mutations.

   (i)   Each cluster center encoded in a string is replaced with a random variable drawn from a Laplacian distribution, $p\left(\in\right)\alpha e^{-\frac{|\in-\mu|}{\delta}}$, where the scaling factor δ sets the magnitude of perturbation. Here μ is the value at the position which is to be perturbed. The scaling factor δ is chosen equal to 1.0. The old value at the position is replaced with the newly generated value. Here this type of mutation operator is applied for all dimensions independently.

   (ii)   Total *C* number of sub-cluster centers are removed from the string, i.e., total number of clusters present in that string is decreased by 1.

   (iii)   The total number of clusters present in that chromosome is increased by 1. *C* randomly chosen points from the data set are encoded as the new sub-cluster centers.

Any one of the above mentioned types of mutation is applied randomly on a particular string if it is selected for mutation.

3.5 Selection of the Best Solution
In MOO, the algorithms produce a large number of non-dominated solutions Deb (2001) on the final Pareto optimal front. Each of these solutions provides a way of clustering the

given data set. All the solutions are equally important from the algorithmic point of view. But sometimes the user may want only a single solution. Consequently, in this paper a method of selecting a single solution from the set of solutions, is now developed. Here the clustering results have been evaluated objectively, i.e., by measuring the goodness of the clusters. For this purpose, an existing well-known cluster validity index is used. The XB-index Xie and Beni (1991) has been proposed as a measure of indicating the goodness/validity of a cluster solution. The XB-index is defined as a function of the ratio of the total variation σ to the minimum separation *sep* of the clusters. Here σ and *sep* are written as:

$$\sigma(U,Z;X) = \sum_{i=1}^{K}\sum_{k=1}^{n}\mu_{ik}^{2}d_{e}^{2}(z_{i},x_{k}),$$

and

$$sep(Z) = \min_{i \neq j}\left\{d_{e}(z_{i},z_{j})^{2}\right\},$$

where *U*, *Z* and *X* represent the partition matrix, set of cluster centers and the data set, respectively. The XB-index is then written as

$$XB = \frac{\sigma(U,Z;X)}{sep(Z)} = \frac{\sum_{i-1}^{K}\left(\sum_{k=1}^{n}\mu_{ik}^{2}d_{e}^{2}(z_{i},x_{k})\right)}{n\left(\min_{i \neq j}\left(d_{e}(z_{i},z_{j})^{2}\right)\right)}.$$

Note that when the partitioning is compact and good, the total deviation (_) should be low while the minimal separation (sep) between any two cluster centers should be high. Thus, the objective is therefore to minimize the XB index for achieving the proper clustering. For all the solutions on the final Pareto optimal front, XB-index values are calculated. Then the solution which corresponds to the lowest XB-index is treated as the best solution.

4. EXPERIMENTAL RESULTS

This section provides a description of the image data sets and the experimental results obtained after application of the above mentioned *multicenter-AMOSA* clustering technique for segmenting two remote sensing satellite images of the parts of the cities of Kolkata and Mumbai. The two satellite images are of size 512×512, i.e., the size of the data set to be clustered in all the images is 262144. For these multispectral satellite images, the feature vector is composed of the intensity values at different bands of the image. The parameters of the algorithm are as follows: *Tmax* = 10, *Tmin* = 0:001, α = 0:8, *SL* = 50 and *HL* = 20. The K^{max} is kept equal to 16 and *C*, total number of sub-clusters

per cluster, is kept equal to 10. The proposed *multicenter-AMOSA* produces a large number of solutions on its final Pareto optimal front. Here a single solution is selected as per the method described in Section 3.5. For the purpose of comparison, Fuzzy C-means (FCM) Bezdek (1981) clustering and VGAPS Bandyopadhyay and Saha (2008) (variable string length genetic point symmetry based automatic clustering technique) are also executed on these real-life images.

4.1 SPOT Image of Kolkata

The French satellites SPOT (Systems Probataire d'Observation de la Terre) Richards (1993), launched in 1986 and 1990, carry two imaging devices that consist of a linear array of charge coupled device (CCD) detectors. Two imaging modes are possible, the multispectral and panchromatic modes. The 512_512 SPOT image of a part of the city of Kolkata is available in three bands in the multispectral mode. These bands are:

Band 1 - green band of wavelength 0.50 - 0.59 μ m

Band 2 - red band of wavelength 0.61 - 0.68 μ m

Band 3 - near infrared band of wavelength 0.79 - 0.89 μ m.

Thus, here feature vector of each image pixel composed of three intensity values at different bands. The distribution of the pixels in the feature space of this image is shown in be partitioned into several hyperspherical clusters.

Some important landcovers of Kolkata are present in the image. Most of these can be identified, from a knowledge about the area, more easily in the near infrared band of the input image (Fig. 3). These are the following: The prominent black stretch across the figure is the river *Hooghly*. Portions of a bridge (referred to as the *second bridge*), which was under construction when the picture was taken,

TABLE 1. XB-INDEX VALUES OF THE SEGMENTED MUMBAI AND KOLKATA SATELLITE IMAGES PROVIDED BY MULTICENTER-AMOSA, VGAPS AND FCM-CLUSTERING TECHNIQUES

Index	XB		
	multicenter-AMOSA	VGAPS	FCM
Kolkata SPOT	1.12	1.15	12.22
Mumbai IRS	1.52	1.64	4.67

protrude into the *Hooghly* near its bend around the center of the image. There are two distinct black, elongated patches below the river, on the left side of the image. These are water bodies, the one to the left being *Garden Reach lake* and the one to the right being *Khidirpore dockyard*. Just to the right of these water bodies, there is a very thin line, starting from the right bank of the river, and going to the bottom edge of the picture. This is a canal called the *Talis nala*. Above the *Talis nala*, on the right side of the picture, there

is a triangular patch, the race course.

On the top, right hand side of the image, there is a thin line, stretching from the top edge, and ending on the middle, left edge. This is the *Beleghata canal* with a road by its side. There are several roads on the right side of the image, near the middle and top portions. These are not very obvious from the images. A bridge cuts the river near the top of the image. This is referred to as the *first bridge*.

The proposed *multicenter-AMOSA* clustering method provides total 12 solutions on the final Pareto front. The best partitioning identified by the method proposed in Section 3.5 corresponds to the solution providing $K = 7$ (corresponding partitioning is shown in Figure 5). As identified in Pal *et al.* (2001) the above satellite image has seven classes namely, *turbid water, concrete, pure water, vegetation, habitation, open space and roads* (including bridges). The partitioning provided by the multicenter-AMOSA clustering technique separates almost all the regions well. The *Talis nala* has been identified properly by the proposed method (shown in Figure 5). The bridge is also correctly identified by the proposed algorithm. This again shows that the proposed *multicenter-AMOSA* (AMOSA based general automatic clustering technique with point symmetry based distance) is able to detect clusters of widely varying sizes. The segmentation result obtained by Fuzzy C-means algorithm on this image for $K = 7$ (actual number of clusters present in this image data set) is shown in Figure 7. It can be seen from Figure 7 that FCM algorithm is not able to detect the bridge. VGAPS clustering technique automatically determines $K = 6$ number of clusters from this data set. The corresponding partitioning is shown in Figure 6. In order to compare the results quantitatively, the well-known cluster validity index, XB-index Xie and Beni (1991) values are also calculated for the partitionings provided by *multicenter-AMOSA* clustering technique, FCM clustering technique and VGAPS clustering technique. The results are reported in Table 1. XB-index is a well-known Euclidean distance based cluster validity index. The smaller values of XB-index correspond to good partitioning. Table 1 shows that *multicenter-AMOSA* clustering technique performs the best compared to FCM and VGAPS clustering techniques according to XB-index values.

4.2 IRS Image of Mumbai

The IRS image of Mumbai was obtained using the LISS-II sensor. It is available in four bands, viz., blue, green, red and near infra-red. Fig. 8 shows the *IRS image* of a part of the city of Mumbai in the near infra red band. As can be seen, the elongated city area is surrounded on three sides by the Arabian sea. Towards the bottom right of the image, there are several islands, including the well known *Elephanta island*. The dockyard is situated on the south eastern part of Mumbai, which can be seen as a set of three finger like structure. This image has been classified into seven clusters Maulik and Bandyopadhyay (2003).

Seminar on Spatial Information Retrieval, Analysis, Reasoning and Modelling
18th-20th March 2009. ISI-DRTC, Bangalore, India

112

Figure 3. SPOT Image of Kolkata in the Near Infra Red Band with Histogram Equalization.
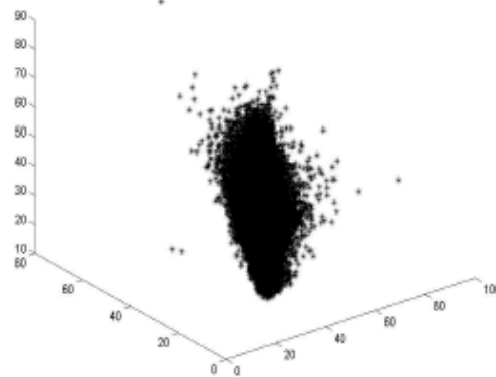
Figure 4. Data distribution of SPOT image of Kolkata in the Feature Space.

The proposed AMOSA based multiobjective clustering technique (multicenter-

AMOSA) provides total 13 solutions on the _nal Pareto optimal front. The partitioning corresponding to the best solution identified by the method proposed in Section 3.5 is shown in Figure 9. Total number of clusters present in this partition is $K = 6$. From the result it can be seen that the large water body of Arabian sea has been distinguished into three classes based on the depth of the sea-water. The islands, dockyard have mostly been correctly identified in the image. The results obtained, for both the Kolkata and Mumbai images are quite encouraging, since the technique has managed to automatically discriminate the classes without any sort of *a priori* knowledge about the data or the number of clusters.

Fig. 11 demonstrates the Mumbai image clustered using the FCM technique when $K = 6$ is given a priori. Again the result is unsatisfactory from the human visualization judgement. It is very difficult to clearly distinguish the Arabian sea from this segmented image (in Figure 11). A significant amount of confusion is evident in the FCM clustering result. The result of the application of the VGAPS clustering technique on the Mumbai image is shown in Fig. 10. The method automatically yielded six clusters.

Figure 5. Clustered SPOT Image of Kolkata Using multicenter-AMOSA Clustering.
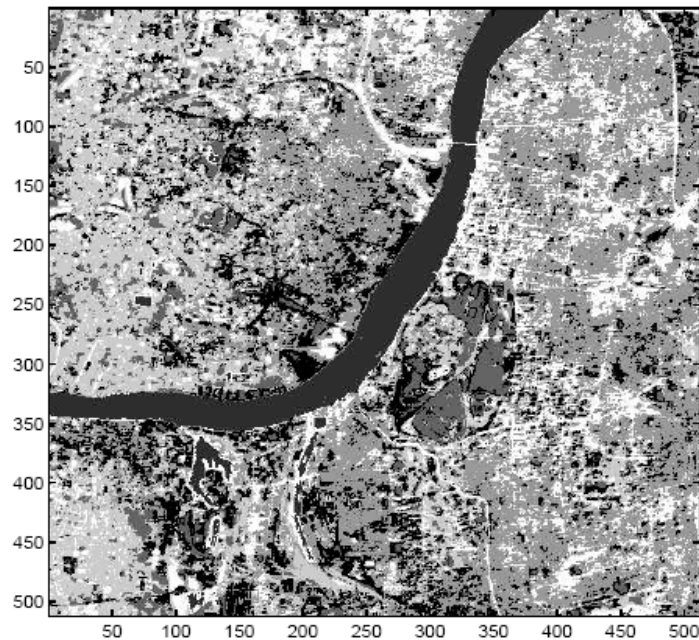
Figure 6. Clustered SPOT Image of Kolkata Using VGAPS Clustering.

In order to compare the results quantitatively the well-known cluster validity index, XB-index values are also calculated for the partitionings provided by *multicenter-AMOSA* clustering technique, VGAPS clustering technique and FCM clustering technique. The results are reported in Table 1. The smaller values of XB- index correspond to good partitioning. Result shown in Table 1 again demonstrates the superior performance of *multicenter-AMOSA* clustering technique.
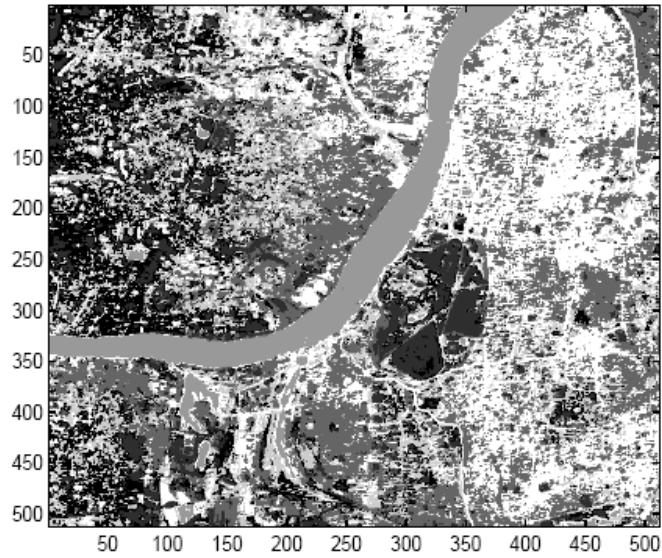
Figure 7. Clustered SPOT Image of Kolkata Using FCM Clustering.
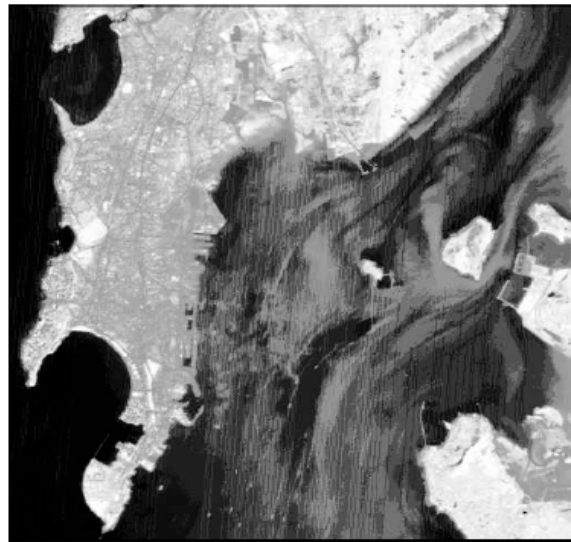
Figure 8. IRS Image of Mumbai in the Near Infra Red Band with Histogram Equalization.

5. DISCUSSION AND CONCLUSIONS

In this article, classification of satellite images into different landcover regions is modeled as the task of clustering the pixels in the intensity space. Consequently a multiobjective clustering technique has been developed for classifying the image. Here in order to represent a particular cluster, multi-center approach has been adopted. Two cluster validity indices are optimized simultaneously. The first objective function reflects total symmetry present in a particular partitioning and the second objective function reflects total degree of compactness of the obtained partitioning. A newly developed multiobjective simulated annealing based technique,

AMOSA, is used as the underlying optimization strategy. Two satellite images of the parts of the cities of Kolkata and Mumbai have been classified using the proposed multiobjective clustering technique and the results are compared with those obtained by the fuzzy C-means and VGAPS clustering techniques. Much further work is needed to investigate using different and more objectives, and to test the approach still more extensively.
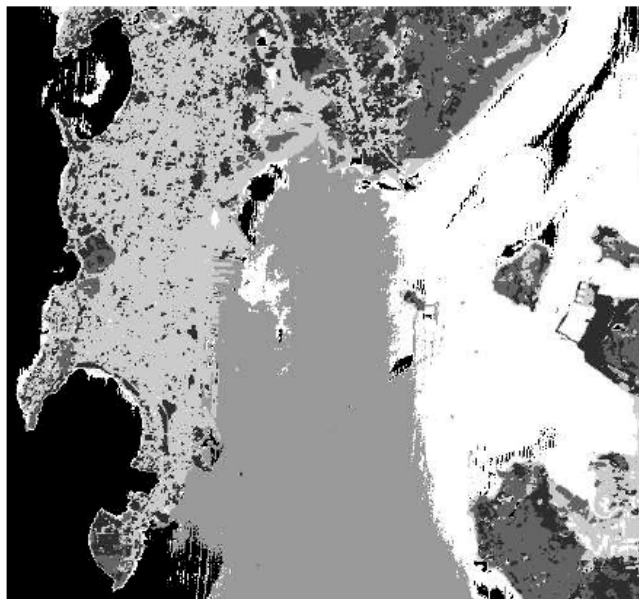
Figure 9. Clustered IRS Image of Mumbai Using multicenter-AMOSA Clustering.
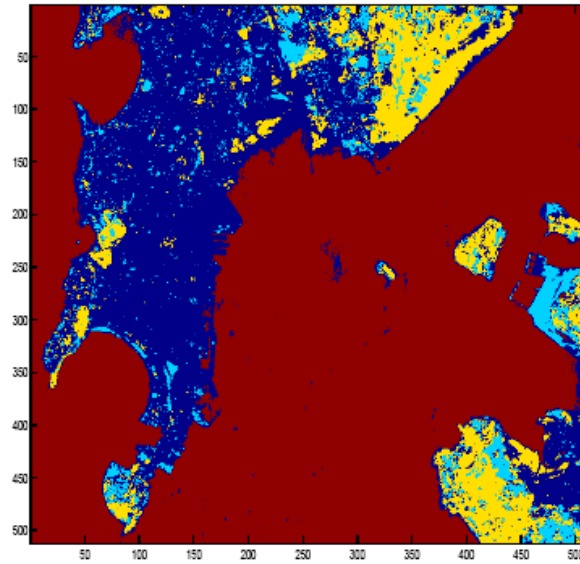
Figure 10. Clustered IRS Image of Mumbai Using VGAPS Clustering.
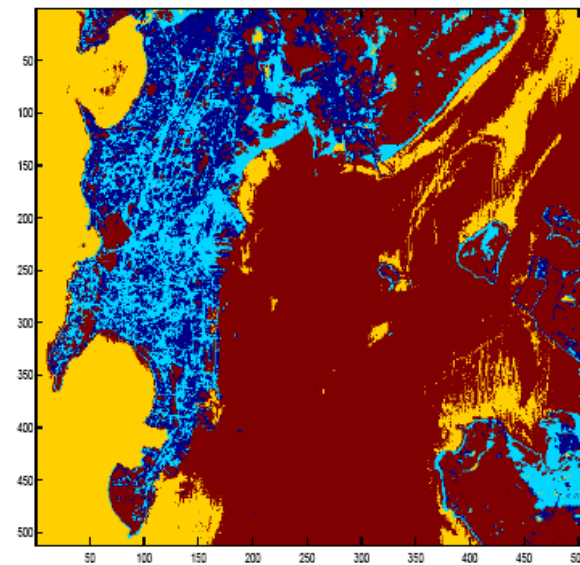
Figure 11. Clustered IRS Image of Mumbai Using FCM Clustering.

REFERENCES

1. Bandyopadhyay, S. and Saha, S., 2007, GAPS: A Clustering Method Using A New Point Symmetry Based Distance Measure. Pattern Recog., 40, pp. 3430-3451.
2. Bandyopadhyay, S. and Saha, S., 2008, A Point Symmetry Based Clustering Technique for Automatic Evolution of Clusters. IEEE Transactions on Knowledge and Data Engineering (accepted).
3. Bandyopadhyay, S., Saha, S., Maulik, U. and Deb, K., JUNE 2008, A Simulated Annealing Based Multi-objective Optimization Algorithm: AMOSA. IEEE Transactions on Evolutionary Computation, 12, pp. 269{283.
4. Bensaid, A.M., Hall, L.O., Bezdek, J.C., Clarke, L.P., Silbiger, M.L., Arrington, J.A. and Murtagh, R.F., 1996, Validity-Guided (Re)Clustering with Applications to Image Segmentation. IEEE Transactions on Fuzzy Systems, 4, pp. 112-123.
5. Bezdek, J.C., 1981, Pattern Recognition with Fuzzy Objective Function Algorithms (New York: Plenum).
6. Deb, K., 2001, Multi-objective Optimization Using Evolutionary Algorithms (England: John Wiley and Sons, Ltd).
7. Deb, K., Pratap, A., Agarwal, S. and Meyarivan, T., 2002, A fast and elitist multiobjective genetic algorithm: NSGA-II. IEEE Transactions on Evolutionary Computation, 6.
8. Everitt, B.S., 1993, Cluster Analysis (Halsted Press, third edition).
9. Geman, S. and Geman, D., 1984, Stochastic Relaxation, Gibbs Distributions and the Bayesian Restoration of Images. IEEE-Transactions on Pattern Analysis and Machine Intelligence, 6, pp. 721-741.
10. Goldberg, D.E., 1989, Genetic Algorithms in Search, Optimization and Machine Learning (New York: Addison-Wesley).
11. Kirkpatrik, S., Gelatt, C. and Vecchi, M., 1983, Optimization by simulated annealing. Science, 220, pp. 671-680.
12. Maulik, U. and Bandyopadhyay, S., 2000, Genetic Algorithm Based Clustering Technique. Pattern Recog., 33, pp. 1455-1465.
13. Maulik, U. and Bandyopadhyay, S., 2002, Performance Evaluation of Some Clustering Algorithms and Validity Indices. IEEE Transactions on Pattern Analysis and Machine Intelligence, 24, pp. 1650-1654.
14. Maulik, U. and Bandyopadhyay, S., 2003, Fuzzy partitioning using a real-coded variable-length genetic algorithm for pixel classi_cation. IEEE Transactions on Geoscience and Remote Sensing, 41, pp. 1075-1081.
15. Pal, S.K., Bandyopadhyay, S. and Murthy, C.A., 2001, Genetic Classifiers for Remotely Sensed Images : Comparison with Standard Methods. International Journal of Remote Sensing, 22, pp. 2545-2569.
16. Richards, J.A., 1993, Remote Sensing Digital Image Analysis : An Introduction (New York: Springer-Verlag).
17. Saha, S. and Bandyopadhyay, S., Accepted, 2007, Fuzzy Symmetry Based Real-Coded Genetic Clustering Technique for Automatic Pixel Classification in Remote Sensing Imagery. Fundamenta Informaticae.
18. Veldhuizen, D.V. and Lamont, G., 2000, Multiobjective Evolutionary Algorithms: Analyzing the State-of-the-Art. Evolutionary Computation, 2, pp. 125-147.
19. Xie, X.L. and Beni, G., 1991, A Validity Measure for Fuzzy Clustering. IEEE Transactions on Pattern Analysis and Machine Intelligence, 13, pp. 841-847.